

Linear phase error correction for improved water and fat separation in the dual-echo Dixon techniques

J. Ma¹, Z. Slavens², W. Sun², E. Bayram², L. Estowski², K-P. Hwang³, J. Akao², and A. T. Vu²

¹Imaging Physics, University of Texas M. D. Anderson Cancer Center, Houston, TX, United States, ²GE Healthcare, Waukesha, WI, United States, ³GE Healthcare, Houston, TX, United States

Introduction: Dual-echo Dixon techniques have been shown to achieve reliable water and fat separation in a similar scan time as the corresponding single-echo technique with conventional fat suppression and otherwise similar scan parameters (1-2). For the actual implementation of a dual-echo Dixon technique, the inter-echo spacing is determined by the desired water and fat relative phase angle. As a result, an increased receiver bandwidth (RBW) and higher amplitude for the readout gradient (Gx) are needed for imaging at high resolution (large number of the frequency encode steps Nx and/or small FOVx) or at increased field strength. While an increased RBW is usually beneficial (e.g., reduced T2* blurring, chemical shift misregistration and geometric distortion), an increased Gx requires large gradient ramp, which in turn may induce large eddy currents. Because the second echo is collected almost immediately after the gradient polarity switch, its center position is particularly susceptible to eddy current induced time shifts that will result in large linear phase errors in the image.

In this work, we propose for processing dual-echo Dixon images a two-step method that first corrects linear phase errors with a modified Ahn-Cho algorithm (3) before applying a region growing based algorithm (1-2) to correct the residual nonlinear components. Both the linear and the region-growing based phase correction algorithms used here do not rely on error-prone phase unwrapping. We demonstrate that successive application of the two algorithms provides a “1-2 punch” to the phase errors and can overcome water and fat separation failures occasionally encountered when the region growing based algorithm is applied alone.

Method: After the Fourier transform, the 180° out-of-phase image is multiplied by the complex conjugate of the in-phase image and then divided by the magnitude of the in-phase image to obtain:

$$S_1(x, y) = (W - F) \cdot e^{i\phi} \quad [1]$$

where ϕ is the relative phase angle between the in-phase and out-of-phase images due to all the factors (field inhomogeneity, echo center offset, etc) other than the chemical shift. x and y are the pixel coordinates along the readout and phase directions, respectively. For data acquired with multiple receiver coils, the complex signal in Eq. [1] can be summed over all the coils without affecting the functional form of the equation and the same phase correction described below will thus still apply.

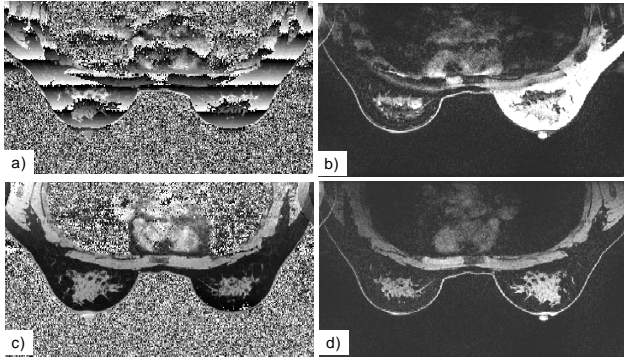
To extract the linear component of the phase error from Eq. [1], we first assume that ϕ is linear in x . We modified the original algorithm by Ahn and Cho (3) to calculate:

$$\mathcal{E}_1 = \arg\left\{ \sum [S_1^2(x, y) \cdot S_1^{2*}(x+1, y)] \right\} \quad [2]$$

where $*$ represents the complex conjugate, $\arg\{ \dots \}$ represents taking the phase argument, and the summation is over all the image pixels. Note that taking the square of S_1 doubles the phase error, but removes chemical shift related phase change. Note also that Eq. [2] is calculated only as a statistical expectation and the result is thus robust with respect to noise, phase wraps, or local artifacts. After \mathcal{E}_1 is determined, we remove the linear phase from S_1 as follows:

$$S_1'(x, y) = S_1(x, y) \cdot e^{-i\mathcal{E}_1 x/2} \quad [3]$$

where the division by 2 in the phase is to compensate the effect of taking the squares in Eq. [2]. Once the linear phase is removed, we use S_1' as the input to the original region growing based algorithm (1-2) to determine the residual non-linear component of the phase errors in Eq. [1]



Experiments and Results: We implemented the above algorithm on a 3.0T Signa® HDx whole body MRI scanner (GE Healthcare, Waukesha, WI) with a prototype gradient system (SR=200, max amplitude=5G/cm). A 3D fast dual-echo spoiled gradient echo pulse sequence was used to collect all the data. The linear phase correction algorithm was evaluated on three sets of high-resolution data (one bilateral axial breast acquired with the following parameters: matrix=160x432x88, FOV=23x35cm, slice thickness=1.8mm, RBW=±167kHz, TE=1.6/2.7ms, TR=4.9ms and total acquisition time=54s using an auto-calibrated parallel imaging method with a net acceleration factor of 2.6; and two coronal abdomen/pelvis with the following parameters: matrix = 320x192x48, FOV=48x38cm, slice thickness=4.0mm, RBW=±167kHz, TE=1.2/2.4ms, TR=4.1ms and total acquisition time=31s with no parallel imaging acceleration). These datasets were selected because water/fat separation failure was noted when the region-growing based algorithm was applied alone. Water and fat images were reconstructed with and without the linear phase error correction and then visually evaluated.

Without the linear phase correction, local water/fat separation failures were observed in all 88 slices for the breast dataset and 41 out of 192 slices for the abdomen/pelvis datasets. With the linear phase correction, successful water/fat separation was achieved for all slices in all datasets. The figures above illustrate a representative slice from the breast dataset. Fig. a) is the phase map before the linear phase correction. For this particular dataset, readout was selected to be along the A/P direction to avoid the chest motion artifacts and the smaller readout number (Nx=160) (compared to Ny=432 along the L/R direction) was useful for the larger lateral coverage needed. However, the small Nx in this case probably contributed to the large linear phase errors seen in Fig. a). With only the region-growing based phase correction, the water-only image in Fig. b) showed several regions of water/fat separation failure. The phase map in Fig. c) shows that the linear phase error was largely corrected after the linear phase correction. The residual phase errors were subsequently removed by the region-growing based algorithm, leading to the clean water-only image in Fig. d).

Discussions: The spatial dependence of the phase errors in Dixon images are in general quite complex. However, linear phase errors are directly induced by several factors, such as eddy currents, data acquisition window offset, system delay or erroneous linear shimming). For dual-echo data acquisition utilizing large gradient ramps, eddy current induced echo shifts are difficult to predict and eliminate. Irrespective of the underlying causes, unusually large linear phase errors may present challenges if the region-growing based phase correction is applied alone. Our results showed that the linear phase correction algorithm can be applied as a first-pass treatment of the phase errors to improve the processing reliability for data acquired in the dual-echo Dixon techniques. It should be noted that the linear phase error determination in Eqs. [1-3] does not even need to be exact since any residual phase errors are handled by the subsequent region-growing based algorithm without affecting the final water/fat separation. Such an approach can be extended to processing other types of the Dixon data (including data acquired with more than two echoes) and has in fact been previously reported (albeit only in the context of more error-prone phase unwrapping) (4).

References: (1) Ma J, MRM 52:415, 2004. (2) Ma J, et. al., JMRI 23 :36, 2006. (3) Ahn CB et.al., IEEE TMI 6:32, 1987. (4) An L, et. al. IEEE TMI 19 :805, 2000.